RADIAL BASIS FUNCTIONS COLLOCATION METHODS FOR MODEL BASED LEVEL-SET SEGMENTATION

A. Gelas, J. Schaerer, O. Bernard, D. Friboulet, P. Clarysse, I.E. Magnin, R. Prost

CREATIS, INSA de Lyon, UCB, CNRS UMR 5220, Inserm U630, France

ABSTRACT

We consider a recent parametric level-set segmentation approach where the implicit interface is the zero level of a continuous function expanded onto compactly supported radial basis functions, defined by their centers, coefficients and supports. We propose to introduce prior knowledge of the shape to be recovered by placing the centers *quasi-uniformly* over an uncertainty area.

Index Terms— Segmentation, Parametric Level-Set, Compactly Supported Radial Basis Functions, Model-Based.

1. INTRODUCTION

Image segmentation remains a challenging task required in many applications, in particular in medical imaging, where different imaging modalities such as PET, CT, MR or ultrasound imaging provide a wide range of image processing problems. Fully automated image processing is critical for conducting large medical investigations or providing quantitative information in routine examinations.

Over the last decades, research in segmentation has been extremely active, especially in medical imaging. It still is a very difficult problem, its success often relies on the use of strong priors of shape and appearance. In most cases the shape of the anatomic feature is approximatively known, or some statistics regarding the shape can be extracted. Such knowledge can be used, as well, to construct a geometrical and statistical *a priori* model of the anatomical feature of interest.

Among segmentation methods, active-contours appear to be one of the best suited for model based applications. These methods consist in capturing a shape by propagating an interface which evolves according to the solution of a Partial Differential Equation (PDE). Differences between approaches reside in the interface representation and in the forces which deform the interface along iterations. The interface can be represented explicitly as with snakes [1], or implicitly like in level-set approaches.

Since their introduction [2], level-set approaches have been implemented by finite-differences on the whole domain, or on a restricted area around the implicit interface. Recently in [3], authors proposed a new approach which can be seen as a *parametric level-set*, where the implicit interface is continuous and represented by a set of parameters corresponding to the expansion coefficients of the implicit function on a set of compactly supported radial basis functions (CSRBF). This new formalism for level-set approaches provides a much more flexible framework, where geometrical constraints can be directly added into the representation itself.

In this paper, we propose the introduction of *a priori* knowledge into this new approach. On the one hand, we restrict the investigation domain to a region of interest around the given d dimensional model interface. On the other hand, we adapt the set of CSRBF to this investigation domain in order to get the best trade-off between the approximation order of the implicit function and robustness of the level-set through its evolution.

2. CSRBF COLLOCATION BASED LEVEL SET METHODS

In the level-set formalism, the interface Γ in $\mathbb{R}^d$ is represented as the zero level-set of a continuous function f of dimension $d+1$, satisfying:

$$\begin{cases} f(\boldsymbol{p},t) > 0, & \text{for } \boldsymbol{p} \in \Omega_{in}(t), \\ f(\boldsymbol{p},t) < 0, & \text{for } \boldsymbol{p} \in \Omega_{out}(t), \\ f(\boldsymbol{p},t) = 0, & \text{for } \boldsymbol{p} \in \partial\Omega_{in}(t) = \Gamma(t)\ . \end{cases}$$

where, considering an open region Ω in $\mathbb{R}^{d+1}$, Ω_{in} is a region in Ω bounded by Γ. Ω_{out} is defined as $\Omega_{out} = \Omega \setminus \Omega_{in}$.

The problem of segmenting an object is typically handled by the evolution of one level-set according to the following general equation:

$$\frac{\partial f(\boldsymbol{p},t)}{\partial t} + \langle \boldsymbol{V}(\boldsymbol{p},t), \boldsymbol{\nabla} f(\boldsymbol{p},t) \rangle = 0, \qquad (1)$$

where $\langle \cdot,\cdot \rangle$ denotes the standard dot product, and $\boldsymbol{V}$ is a velocity vector field that could originate from an energy minimization process, or that could be provided directly by the user.

In [3], authors decompose the implicit function f on a basis of CSRBFs:

$$f(\boldsymbol{p}) = \sum_{i=0}^{N-1} \alpha_i \cdot \boldsymbol{\phi}\left(\frac{\|\boldsymbol{p} - \boldsymbol{c}_i\|}{\sigma}\right), \forall\, \boldsymbol{p} \in \Omega \qquad (2)$$

where $\boldsymbol{\phi} = \boldsymbol{\phi}_{d,k}$ is a CSRBF [4] (d is the dimension and k is the desired continuity order), σ is the support size, $\mathcal{C} = \{\boldsymbol{c}_i\}_{i=0}^{N-1}$ is the set of CSRBF centers, and $\boldsymbol{\alpha} = \{\alpha_i\}_{i=0}^{N-1}$ are CSRBF coefficients. Then they assume that the solution of the level-set PDE (Eq.1) is space and time separable, i.e. the time dependence of f is only due to the CSRBF coefficients:

$$f(\boldsymbol{p},t) = \sum_{i=0}^{N-1} \alpha_i(t) \cdot \boldsymbol{\phi}_i(\boldsymbol{p}),\ \boldsymbol{\phi}_i(\boldsymbol{p}) = \boldsymbol{\phi}\left(\frac{\|\boldsymbol{c}_i - \boldsymbol{p}\|}{\sigma}\right) \quad (3)$$

Substituing Eq.3 into Eq.1 yields an Ordinary Differential Equation (ODE) for CSRBF coefficients which applies to any point $\boldsymbol{p}$ of the domain Ω. In order to solve the level-set evolution, this equation has to be sampled at N distinct points that were chosen to be the CSRBF centers. This leads to solve the following ODE:

$$H \cdot \frac{d\boldsymbol{\alpha}(t)}{dt} = -\boldsymbol{B}(\boldsymbol{\alpha}(t),t), \quad (4)$$

where $H_{ij} = \boldsymbol{\phi}_i(\boldsymbol{c}_j)$ is a $N \times N$ sparse matrix, and $\boldsymbol{B}(\boldsymbol{\alpha}(t),t)$ is a column vector related to the level-set formalism used in Eq.1:

$$\begin{aligned}\left[\boldsymbol{B}(\boldsymbol{\alpha}(t),t)\right]_i &= \langle \boldsymbol{V}(\boldsymbol{p}_i,t), \boldsymbol{\nabla}\boldsymbol{\Phi}(\boldsymbol{p}_i)\cdot\boldsymbol{\alpha}(t)\rangle \\ \boldsymbol{\nabla}\boldsymbol{\Phi}(\boldsymbol{p}) &= \left[\boldsymbol{\nabla}\boldsymbol{\phi}_0(\boldsymbol{p}),\ldots,\boldsymbol{\nabla}\boldsymbol{\phi}_{N-1}(\boldsymbol{p})\right]\end{aligned}$$

By using the conventional forward Euler method, the resolution of this ODE amounts to solve the following linear system:

$$\boldsymbol{\alpha}^{n+1} = \boldsymbol{\alpha}^n - \tau \cdot H^{-1} \cdot \boldsymbol{B}^n(\boldsymbol{\alpha}^n), \quad (5)$$

with τ the step size.

Finally at each iteration, the following algorithm results

$$\begin{cases} L \cdot \boldsymbol{u}^n = B^n(\tilde{\boldsymbol{\alpha}}^n) & (6)\\ L^T \cdot \boldsymbol{v}^n = \boldsymbol{u}^n & (7)\\ \boldsymbol{\alpha}^{n+1} = \tilde{\boldsymbol{\alpha}}^n - \tau \cdot \boldsymbol{v}^n & (8)\\ \tilde{\boldsymbol{\alpha}}^{n+1} = \dfrac{\beta}{\|\boldsymbol{\alpha}^{n+1}\|_1} \cdot \boldsymbol{\alpha}^{n+1}, \qquad if \|\boldsymbol{\alpha}^{n+1}\|_1 > \beta & (9)\end{cases}$$

where β is a normalization factor. The last operation in Eq.9 is presented as a constraint on the implicit function value and gradient norm value during the evolution of the implicit interface Γ_0.

3. OUR CONTRIBUTION

3.1. Introduction

In [3], the authors propose to locate CSRBF centers on a d-dimensional regular grid (i.e. a regular square grid) whenever no prior information about the shape to be recovered is provided. The CSRBF support size is then deduced from the center distribution.

Due to the iterative method used in [3], the H matrix should be well-conditionned in order to avoid large numerical errors at each iteration.

Definition 1. *The* separation distance *of a given point set* $\mathcal{P} = \{\boldsymbol{p}_i\}_{i=0}^{N-1}$ *is defined as follows:*

$$q_{\mathcal{P}} = \frac{1}{2}\min_{i\neq j}\|\boldsymbol{p}_i - \boldsymbol{p}_j\|.$$

Definition 2. *The* fill distance *of a given point set* $\mathcal{P} = \{\boldsymbol{p}_i\}_{i=0}^{N-1}$ *in a given domain* Ω *is defined as follows:*

$$h_{\mathcal{P},\Omega} = \sup_{\boldsymbol{p}\in\Omega}\min_{\boldsymbol{p}_j\in\mathcal{P}}\|\boldsymbol{p} - \boldsymbol{p}_j\|$$

Definition 3. *A given point set* $\mathcal{P} = \{\boldsymbol{p}_i\}_{i=0}^{N-1}$ *is said to be* quasi uniform *with respect to a constant* c_{qu} *if*

$$q_{\mathcal{P}} \leqslant h_{\mathcal{P},\Omega} \leqslant c_{qu} \cdot q_{\mathcal{P}}$$

According to [5], a *quasi-uniform* center set $\mathcal{C}$ with an appropriate support size, i.e. $\sigma = k \cdot h_{\mathcal{C},\Omega}$, provides an excellent trade-off between the approximation order for the implicit function f and the condition number of H.

Thus, we propose here a new and original method to find an adapted center distribution which ensures its *quasi uniformity*, where the domain Ω is chosen according to a given model in any dimension d.

3.2. Statement

We consider that the model is expressed by an implicit function f_0 and its corresponding implicit interface Γ_0, that could be provided by a shape model, an atlas or by any implicit interface reconstruction method [6, 7].

First, we define the domain Ω according to the model implicit function. We assume that the object to be segmented is not too far from the given model interface. To this end, we define an uncertain area which corresponds to the maximal admissible distance from the model to the object to be segmented. Then, all centers $\boldsymbol{c}_i$ should be located inside this uncertainty area, which is determined by setting the parameter D in Eq.10.

In order to produce a *quasi uniform* center set $\mathcal{C}$ in Ω, we impose the distance to the closest center for each center $\boldsymbol{c}_i$ (Eq.11).

The algorithm should satisfy the two following constraints:

$$\begin{cases} |f_0(\boldsymbol{c}_i)| \leqslant D & (10)\\ \min\limits_{\boldsymbol{c}_j\in\mathcal{C}}\|\boldsymbol{c}_i - \boldsymbol{c}_j\| = R & (11)\end{cases}$$

where D and R are fixed positive parameters.

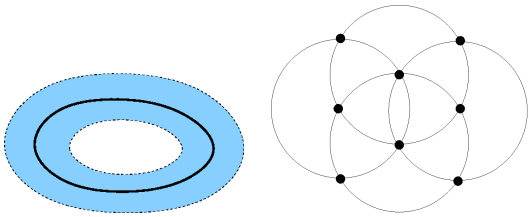

(a) (b)

Fig. 1. The uncertainty area (a) is represented in blue (its thickness is $2 \cdot D$). A few centers are represented such that their closest neighbor is at a distance of R (b).

3.3. Proposed Algorithm

In order to fulfill both conditions (Eq.10-11), we propose an algorithm in the spirit of [8].

Consider a given implicit function f_0, and a given d dimensional grid I on which f_0 is sampled. Depending on the implicit function value at its corresponding location $\boldsymbol{p}$, one grid node n is labelled, by the LABELELEMENTS procedure, as ALIVE (if $|f_0(\boldsymbol{p})| < D$), or DEAD.

We select one node u from the border between ALIVE and DEAD labelled elements, via the SELECTNODE procedure. The corresponding location $\boldsymbol{p}$ of this node is added to the center set $\mathcal{C}$. Then, all ALIVE nodes n such that the euclidean distance to u is below R are labelled as DEAD by the KILLNODES procedure. These last processes are iteratively repeated until there are no more ALIVE nodes. The algorithm is summarized in Algorithm 1 and illustrated in Fig.2.

Algorithm 1 Compute Centers (f_0, D, R, I)

```
1: procedure COMPUTECENTERS(f_0, D, R, I)
2:     C ← ∅
3:     ALIVE, DEAD ← LABELELEMENTS(f_0,I,D)
4:     repeat
5:         u ←SELECTNODE(ALIVE, DEAD)
6:         C ← C ∪ {u}
7:         KILLNODES(u,R,ALIVE, DEAD)
8:     until Card(ALIVE) = 0
9: end procedure
```

4. RESULTS AND DISCUSSION

We have implemented the proposed method for any dimension d. Here we present some results for $d = 2$ and 3.

4.1. 2D Case

In order to illustrate our proposed method, we consider a sample numerical model of a mouse foetus (see Fig.3(a)). The corresponding implicit function f_0 has been created by applying a 2D version of [7].

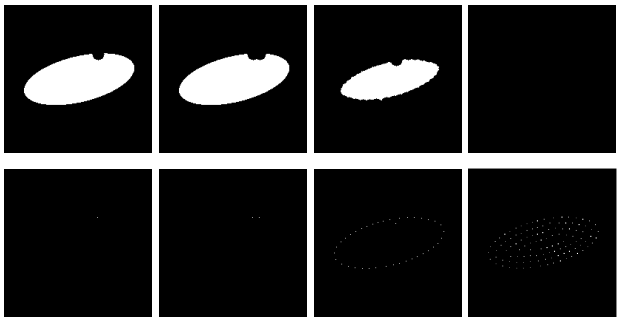

Fig. 2. The top row shows nodes labelled as ALIVE, with the corresponding center set $\mathcal{C}$ on the bottom row, at different iteration steps.

Center distribution

Fig.3(b) shows the center distribution inside the investigation domain Ω next to its zero set. It shows that the constraint on the distance from one center to its closest neighbor holds, and the quasi-uniformity of the center set in Ω. Note that our proposed method can be used for disconnected components, various topologies, and non-convex elements, as well.

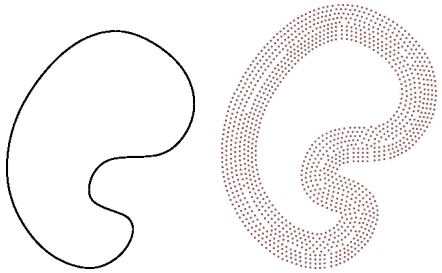

(a) (b)

Fig. 3. Numerical mouse foetus contour model (a). Center distribution (b) inside the investigation domain Ω satisfying constraints in Eq.10-11.

Segmentation

From the constructed implicit function f_0, used as an initialization for the segmentation, we apply the process presented in section 2, more precisely Eq.6-9 in order to extract the synthetic foetus model on the 2D numerical simulation.

Eq.1 requires that a velocity function $\boldsymbol{V}(\boldsymbol{p}, t)$ be derived from the image data, in order to drive the interface towards the image contours. Since we sample the function at the centers' locations on the whole investigation domain Ω (not only near the interface), we must ensure that the direction of the velocity term stays consistent inside Ω. One method that provides a consistent velocity field even far from the interface is the GVF [9]. Fig.4 shows an example of segmentation using the GVF on a synthetic model.

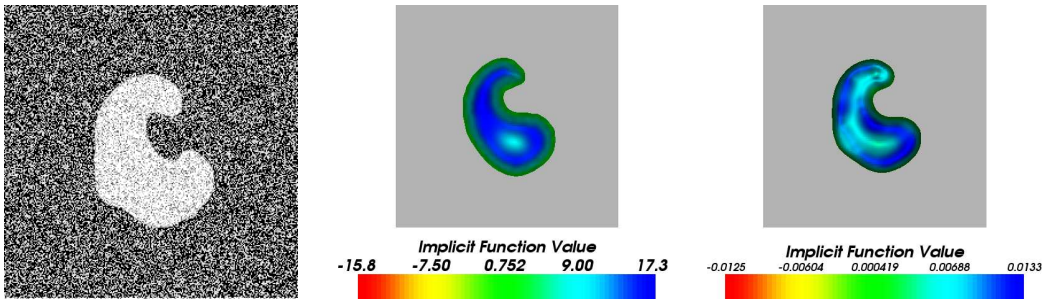

(a) (b) (c)

Fig. 4. Sample segmentation results: The synthetic mouse foetus image to be segmented (a); Initialization of the implicit function (b) according to the foetus model (Fig.3(a)); Resulting implicit function (c).

4.2. Center distribution over a 3-dimensional domain

In order to show the potential of our method in 3D, we applied it to a 3D synthetic model with two cavities. The resulting placement of centers can be seen on Fig.5.

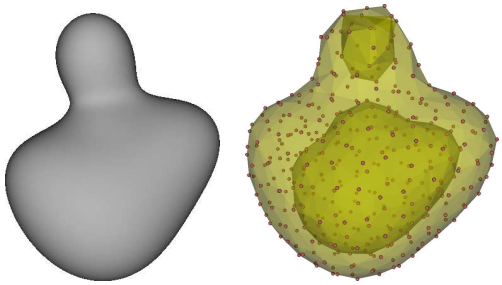

(a) (b)

Fig. 5. On the left, 3D synthetic model with two cavities and non-convex borders. On the right, placement of centers inside an uncertainty zone near the model.

4.3. Discussion

We have presented a novel algorithm for center placement in a model-based parametric level-set framework and some results on synthetic data. Further work will include the use of this method to place CSRBF centers, and the validation on real medical data using existing models.

5. ACKNOWLEDGEMENTS

This work was supported by the "Région Rhône-Alpes", with the EURODOC program, the Cluster project I3M, the *Fondation pour la Recherche Médicale*, the ACI-AGIR and the ANR-GWENDIA projects.

6. REFERENCES

[1] M. Kass, A. Witkin, and D. Terzopoulos, "Snakes: Active contour models," *International Journal of Computer Vision*, vol. 1, no. 4, pp. 321–331, 1988.

[2] S. Osher and J.A. Sethian, "Fronts propagating with curvature-dependent speed: algorithms based on Hamilton-Jacobi formulations," *Journal of Computational Physics*, vol. 79, no. 1, pp. 12–49, 1988.

[3] A. Gelas, O. Bernard, D. Friboulet, and R. Prost, "Compactly supported radial basis functions based collocation method for level-set evolution in image segmentation," *IEEE Trans. on Image Processing*, 2007, (in press).

[4] H. Wendland, "Piecewise polynomial, positive definite and compactly supported radial basis functions of minimal degree," *Adv. Comput. Math.*, vol. 4, pp. 389–396, 1995.

[5] H. Wendland, *Scattered data approximation*, Cambridge University Press, 2005.

[6] Y. Ohtake, A. Belyaev, and H.-P. Seidel, "A multi-scale approach to 3d scattered data interpolation with compactly supported basis functions," in *IEEE SMI 2003*, Seoul, Korea, 2003, pp. 153–161.

[7] A. Gelas, Y. Ohtake, T. Kanai, and R. Prost, "Approximation of unorganized point set with composite implicit surface," in *IEEE ICIP'06*, Atlanta, 2006, pp. 1217–1220.

[8] J. Lotjonen, P.J. Reissman, I.E. Magnin, J. Nenonen, and T. Katila, "Triangulation method of an arbitrary point set for biomagnetic problems," *IEEE Trans. Magnetics*, vol. 34, no. 4, pp. 2228–2233, 1998.

[9] C. Xu and J. L. Prince, "Snakes, shapes, and gradient vector flow," *IEEE Trans. on Image Processing*, vol. 7, pp. 359–369, 1998.